COMMUNICATION

This is the accepted version of the following article: Chem. Commun., 2022, 58, 7495 – 7498, which has been published in a final form at
https://doi.org/10.1039/D2CC02612K

Received 00th January 20xx,
Accepted 00th January 20xx

DOI: 10.1039/x0xx00000x

Cross-linkable Carbazole-Based Hole Transporting Materials for Perovskite Solar Cells

Sarune Daskeviciute-Geguziene,[a] Artiom Magomedov,[a,b] Maryte Daskeviciene,[a] Kristijonas Genevičius,[c] Nerijus Nekrašas,[c] Vygintas Jankauskas [c], Kristina Kantminiene,[d] Michael D. McGehee[b] and Vytautas Getautis*[a]

Carbazole-based molecules V1205 and V1206 capable of cross-linking via three vinyl groups were synthesized by a simple process and applied as hole-transporting materials (HTMs) in inverted perovskite solar cells (PSC). Novel HTMs were thermally polymerized to provide films resistant to organic solvents. A PSC with V1205 exhibited a photovoltaic conversion efficiency of 16.9% with good stability.

Organic–inorganic hybrid perovskite solar cells (PSCs) have been attracting increasing worldwide attention as a competitive alternative to conventional silicon-based solar cells [1] owing to their low-cost constituent materials, solution processing [2] and high power conversion efficiencies (PCEs) [3]. Currently, the highest PCE of 25.8% (certified 25.5%) under standard illumination published in peer-reviewed journals was achieved in a so-called “regular”, or n-i-p configuration, where HTM is deposited on top of the perovskite absorber layer [4]. As an alternative, in recent years, also p-i-n (or “inverted”) configuration of PSCs has been explored with efficiencies getting close to those of the best regular PSCs (the highest published PCE value is 25.0%) [5]. Moreover, inverted PSCs have an advantage in tandem applications where atomic layer deposition of SnOx if often used to provide a functional protective contact that enables sputtering of transparent conducting oxides [6]. The advantages of PSCs with the inverted p-i-n architecture over n-i-p ones include the possibility of low-temperature processing, absence of dopants in the hole transporting layer, negligible hysteresis behavior, and compatibility with organic electronics manufacturing processes [7]. However, in the case of p-i-n devices, solution-processing of the perovskite absorber layer adds additional constraints on the choice of HTMs, as it usually should withstand a mixture of polar DMF:DMSO solvents. Therefore, so far the most popular choice of organic HTMs for such devices are polymers, such as PEDOT:PSS [8] and PTAA [9], or combination of them [10]. As an alternative, several strategies have been reported, e.g. use of self-assembled monolayers [11], change of the perovskite precursor solvent [12] or use of soluble precursors that are subsequently transformed into insoluble films [13]. Recently, cross-linkable fluorene-based HTMs have been introduced into inverted PSCs devices resulting in relatively high performances [14]. These small-molecule-based HTMs can be *in situ* converted into solvent-resistant, cross-linked networks. This approach provides an ideal solution to avoid tedious synthesis and purification that are often encountered for polymers.

On the other hand, the low-cost 9*H*-carbazole as a starting material is interesting due to its excellent charge-transport properties, high chemical stability, and simple functionalization of the structure with a variety of functional groups, which enable fine-tuning of the optical and electronic properties of target HTMs [15]. Therefore, carbazole-based derivatives have been employed in organic light-emitting diodes [16], organic thin film transistors [17], and dye-sensitized solar cells [18]. In recent years, carbazole-based HTMs have also attracted much attention in perovskite solar cells [19].

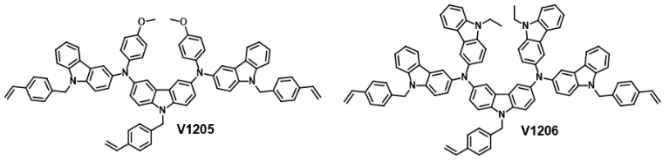

Fig. 1 Molecular structures of the synthesized carbazole-based cross-linkable HTMs **V1205** and **V1206**.

In this work, cross-linkable carbazole-based HTMs **V1205** and **V1206** (Fig. 1), containing three vinyl groups, were synthesized in the simple reactions from commercially available materials and their properties were investigated. The new compounds

[a] *Department of Organic Chemistry, Kaunas University of Technology, Kaunas 50254, Lithuania.*
***E-mail**: vytautas.getautis@ktu.lt*
[b] *Department of Chemical and Biological Engineering, University of Colorado, Boulder, CO, 80309 USA*
[c] *Institute of Chemical Physics, Vilnius University, Vilnius 10257, Lithuania.*
[d] *Department of Physical and Inorganic Chemistry, Kaunas University of Technology, Kaunas 50254, Lithuania.*
Electronic Supplementary Information (ESI) available. See DOI: 10.1039/x0xx00000x

underwent thermal polymerization to form solvent-resistant films. As a proof of concept, PSCs of p-i-n configuration were

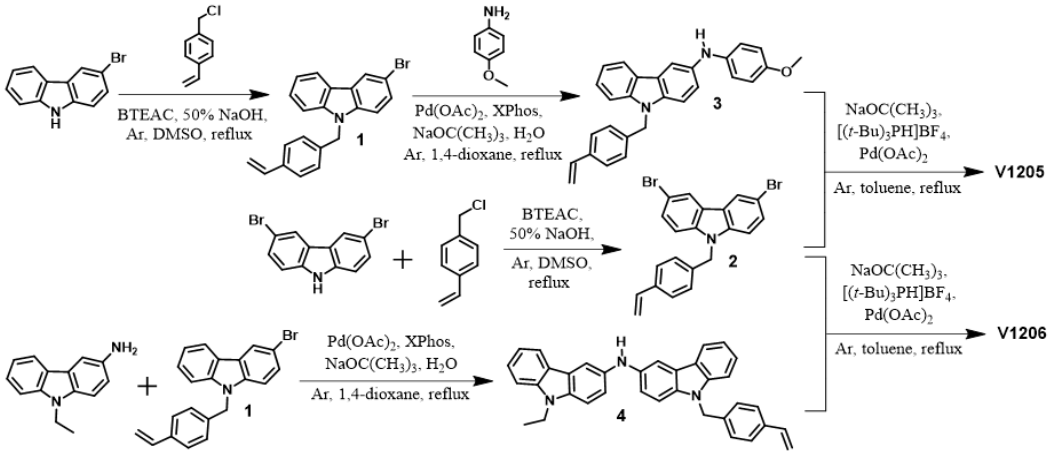

Scheme 1. Synthetic route to **V1205** and **V1206**.

constructed, and a promising PCE of 16.7% was reached for a device with polymerized **V1205**, indicating a great potential of the presented class of cross-linkable dopant-free HTMs.

For the target materials to undergo *in situ* cross-linking, it is required to incorporate at least two groups that can undergo polymerization into the structure of the final cross-linked networks. Therefore, commercially available 3-bromo-9*H*-carbazole and 3,6-dibromo-9*H*-carbazole were chosen as starting compounds and two precursors **1** and **2** were synthesized by using a simple alkylation reaction scheme (Scheme 1). Next, in a sequential Hartwig-Buchwald palladium-catalyzed amination, *p*-anisidine was first coupled with **1** to yield compound **3**, which was then reacted with precursor **2** to provide the target product **V1205** containing three cross-linking 4-vinylbenzyl groups**.** Similarly, the precursor **1** reacted with 3-amino-9-ethylcarbazole to produce compound **4**, which could be treated with compound **2** to provide the final product **V1206** bearing cross-linking 4-vinylbenzyl groups. **V1206** was designed by replacing 4-methoxyphenyl groups in **V1205** with carbazolyl moieties. Structures of the synthesized compounds were confirmed by NMR and elemental analysis data. Detailed synthesis procedures and analysis data are reported in the ESI.

To evaluate the optical properties of the synthesized compounds, UV/vis and photoluminescence (PL) spectra were recorded from the solutions (Fig. 2a). The UV spectra for both monomers, **V1205** and **V1206**, show an absorption maximum (λ_{max}) in the UV range at 325 nm, while only negligible absorption in the visible range of electromagnetic radiation has been recorded. The latter property is particularly important in devices with a p-i-n architecture, in which the light first passes through the HTM layer. Furthermore, it can be seen from the PL spectra that the emission of **V1206** is slightly red-shifted by 9 nm, compared to that of **V1205**, which corresponds to the increased π-conjugated electron system.

For the evaluation of the thermal stability of the synthesized carbazole-based materials and their ability to undergo a cross-linking process, thermal properties were studied by means of thermogravimetric analysis (TGA) and differential scanning calorimetry (DSC). Both compounds showed excellent thermal stability, with a T_{dec} of 443 °C for **V1205** and 404 °C for **V1206**, as seen from the TGA analysis (Fig. S1). The DSC curves have shown that both investigated compounds exist only in an amorphous state since no endothermic melting peaks were detected during both heating cycles (Fig. 2b). For **V1205**, during the first DSC heating cycle, the glass transition process was detected at 117 °C, followed by an exothermic process at 196 °C, suggesting that thermal polymerization occurred at this temperature. During the second heating cycle, no phase transitions were observed, confirming the formation of the cross-linked polymer. For compound **V1206**, with higher molecular weight, a lower T_g of 56 °C was detected and the cross-linking process started at ~270 °C with a peak at ~300 °C (Fig. 2b). Again, during the second heating cycle, no phase transitions were detected. It should be noted that this cross-linking process does not require any use of initiators or dopants, and consequently, no unexpected impurities and defects that are detrimental to the device efficiency and stability can be introduced.

To evaluate the cross-linking ability of the thin films of the carbazole-based HTMs, the amount of washed material from the spin-coated film was evaluated by means of UV/vis spectroscopy (detailed cross-linking procedure is provided in the ESI). The results are presented in Figures 2c and 2d. When the film prepared from **V1205** was heated at 200 °C, already after 1 h, most of the monomer was cross-linked

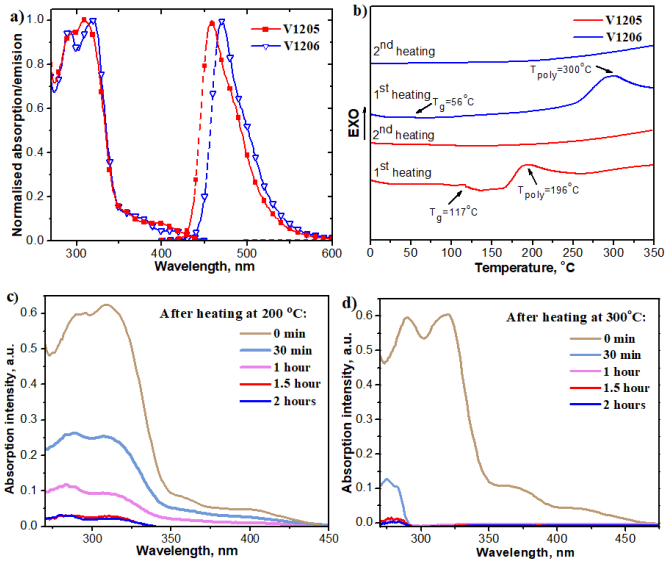

Fig. 2 (a) UV/vs and PL spectra of the solutions of **V1205** and **V1206** (THF, 10^{-4} M); (b) First and second scan heating curves of **V1205** and **V1206** (heating rate 10 °C min^{-1}, the y-axis is showing a heat flux). Cross-linking experiment of **V1205** (c) and **V1206** (d) films. The UV/vis spectra of the solutions prepared by dipping spin coated HTM films into THF after heating at 200 °C (c) and 300 °C (d) for the respective duration.

into an insoluble polymer while in the case of **V1206** this process was faster – it took only 30 min. For both films, the cross-linking was completed roughly after 1.5 h of heating. The cross-linked films have shown to be resistant to the DMF:DMSO (4:1) solvent mixture, as after exposure to them the UV/vis absorption spectra of the films remained almost the same (Figure S7 and Figure S8).

Next, the ability of new HTMs to transport charges was evaluated by the xerographic time-of-flight (XTOF) technique. The measured electric field dependencies of the hole drift mobilities in **V1205** and **V1206** are presented in Figure 3. For both new HTMs, measurements from pure layers were not possible due to their insufficient quality, therefore, the charge transfer in layers of blends with bisphenol Z-polycarbonate (PC-Z), in weight ratios of 1:1, 1:2 or 1:3, which were

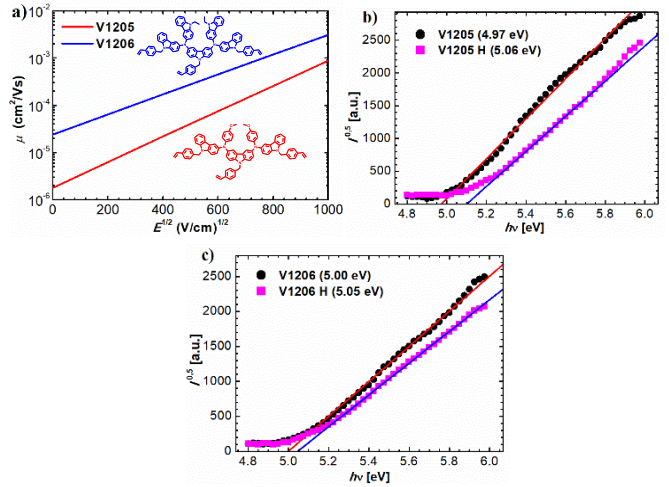

Fig. 3 (a) Charge mobility of **V1205** and **V1206;** (b) UV emission spectra of not heated (**V1205**) and cross-linked (**V1205H**) samples; (c) UV emission spectra of not heated (**V1206**) and cross-linked (**V1206H**) samples.

of suitable quality, were studied in detail (Figure S2-S5). Based on the exponential dependence of the charge carrier mobility on the average distance between the charge transporting molecules [20], interpolated mobility values were calculated for the case of pure material. Compound **V1206** bearing higher number of carbazolyl chromophores showed good charge transporting properties, i.e. reached 10^{-3} cm^2/Vs at strong electrical fields (Fig. 3a). The simpler compound **V1205** showed slightly lower hole drift mobilities, yet still comparable to that of popular HTMs for PSCs. Since the cross-linking process does not affect the chromophoric system of the HTMs, it had only a minor influence on the hole drift mobility. Hole drift mobility of **V1205** even increased slightly after cross-linking (Figure S6), as was confirmed by the time-of-flight (TOF) method, as no measurement results were obtained by the XTOF method. Unfortunately, it was not possible to measure the hole drift mobility of **V1206** after cross-linking using neither the XTOF nor the TOF method. In addition to charge transporting properties, ionization potentials were measured through photoelectron spectroscopy in air (PESA). The values were 4.97 eV and 5.00 eV for **V1205** and **V1206**, respectively (Figures 3b and 3c). As expected, these values changed negligibly after cross-linking (Figures 3b and 3c). The recorded ionization potential values are consistent with the values reported for other HTMs used in PSCs.

To evaluate the performance of materials acting as hole-selective layers in PSCs, devices with p-i-n architecture (Figure 4a) were fabricated and characterized. As an absorber material, triple-cation perovskite was used, with a nominal precursor solution composition of $Cs_{0.05}(FA_{0.83}MA_{0.17})_{0.95}Pb(I_{0.83}Br_{0.17})_3$. The films of the organic HTMs were prepared by spin-coating from toluene followed by the annealing at 200°C (1.5 h) for **V1205** and 300°C (1 h) for **V1206** to achieve cross-linking, as was determined previously. A detailed description of the fabrication and characterization of the devices can be found in the Electronic Supporting Information. The photovoltaic performance of the perovskite solar cells was evaluated from their

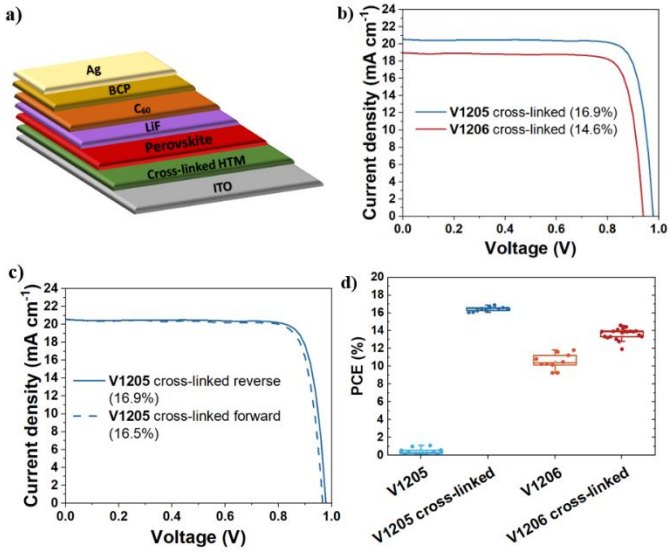

Fig. 4 (a) Architecture of the PSEs; (b) *J*/*V* measurements of the new HTMs (cross-linked), reverse scan; (c) *J*/*V* measurements of the cross-linked **V1205**, showing reverse and forward scans; (d) Statistical distribution of the PCE for the HTMs studied.

Table 1. Performance parameters of the measured devices. The data extracted from *J*/*V* scans (reverse and forward), and includes average with standard deviation, as well as best value (in brackets).

HTM	J_{SC}, mA cm^{-1}	V_{OC}, mV	*FF*, %	*PCE*, %
V1205	14.6±0.5 (15.6)	120±81 (285)	24.5±0.4 (25.1)	0.4±0.3 (1.1)
V1205 cross-linked	20.4±0.2 (20.6)	971±6 (979)	82.8±1.1 (84.4)	16.4±0.2 (16.9)
V1206	18.3±0.2 (18.6)	759±33 (819)	75.7±3.1 (80.8)	10.5±0.8 (11.8)
V1206 cross-linked	18.6±0.2 (19.0)	911±23 (944)	80.4±1.7 (82.3)	13.7±0.6 (14.6)

photocurrent density-voltage (*J*–*V*) characteristics. The cross-linked **V1205** allowed for higher open-circuit voltages (V_{OC}) and current density (J_{SC}) and, as a consequence, the higher PCE of 16.9% than that of **V1206** (Figure 4b, Table 1). As seen from Figure 4c, only minor hysteresis was recorded. Performance of the employing thermally cross-linked HTM films was compared with that of neat films. As presented in Figure 4d, PCE recorded for the devices employing monomer films of **V1206** was lower (by 10.0% on average) compared with that of the devices with crosslinked same HTM. Lowering of PCE can be attributed to the formation of direct contact between perovskite and ITO due to the damage of the HTM film during solution-processing of the perovskite film. This in turn led to an increased interfacial recombination, which reduced Voc. Interestingly, devices with the monomer **V1205** practically did not function. Apparently, the HTM layer was severely damaged in this case. The solubility of both monomers was tested in a DMF and DMSO mixture (4:1) since this mixture of solvents is used during the formation of the perovskite layer. Solubility of monomer **V1205** was almost twice higher (10 mg/ 50 µl) than that of monomer **V1206** (10 mg/ 80 µl) what is in accordance with the obtained results. In order to estimate the stability of the fabricated devices with the best performing cross-linked **V1205**, we have retested the devices after 30 days (N_2 atmosphere, dark, room temperature). Overall, the devices have shown a good shelf lifetime. For the best pixel, 97% of the initial performance was retained. The main reason behind the slightly lower performance was a drop in V_{OC} (Fig. S9), which could be attributed to the increased number of defects in the bulk of perovskite. A more detailed statistical analysis of the aged devices can be found in Table S1.

In summary, two novel carbazole-based hole-transporting materials, namely **V1205** and **V1206**, were synthesized by a simple process with high yield and investigated. The synthesized compounds exhibit good thermal stabilities, high hole-drift mobilities and appropriate HOMO levels, indicating that these materials can be promising HTMs in PSCs. Due to the presence of three vinyl groups, compounds **V1205** and **V1206** are able to undergo thermal cross-linking during the heating at 200 °C and 300 °C, respectively. After thermal polymerization the deposited films became resistant towards organic solvents. By employing cross-linked **V1205** and **V1206** as HTM layers between perovskite and ITO in inverted type perovskite solar cells, the PCE is improved to 16.9% (**V1205**) and to 14.6% (**V1206**) under AM 1.5G 100 mW cm^{-2} illumination. To achieve higher efficiency, further optimization of the concentration of the cross-linkable HTMs is under investigation and will be reported later.

We acknowledge the financial support from the Research Council of Lithuania (grant No. MIP-19-14). A.M. acknowledges funding from the Fulbright Scholar Program.

Notes and references

1 G. Hodes, *Science*, 2013, **342**, 317.
2 Y. Rong, Y. Hu, A. Mei, H. Tan, M. I. Saidaminov, S. Il Seok, M. D. McGehee, E. H. Sargent and H. Han, *Science*, 2018, **361**, 1214.
3 https://www.nrel.gov/pv/cell-efficiency.html, accessed 06-2022.
4 H. Min, D. Y. Lee, J. Kim, G. Kim, K. S. Lee, J. Kim, M. J. Paik, Y. K. Kim, K. S. Kim, M. G. Kim, T. J. Shin and S. I. Seok, *Nature*, 2021, **598**, 444.
5 Z. Li, B. Li, X. Wu, S. A. Sheppard, S. Zhang, D. Gao, N. J. Long, Z. Zhu, *Science*, 2022, **376**, 416.
6 (a) J. Xu, C. C. Boyd, Z. J. Yu, A. F. Palmstrom, D. J. Witter, B. W. Larson, R. M. France, J. Werner, S. P. Harvey, E. J. Wolf, W. Weigand, S. Manzoor, M. F. A. M. Van Hest, J. J. Berry, J. M. Luther, Z. C. Holman and M. D. McGehee, *Science*, 2020, **367**, 1097; (b) Y. Hou, E. Aydin, M. De Bastiani, C. Xiao, F. H. Isikgor, D. J. Xue, B. Chen, H. Chen, B. Bahrami, A. H. Chowdhury, A. Johnston, S. W. Baek, Z. Huang, M. Wei, Y. Dong, J. Troughton, R. Jalmood, A. J. Mirabelli, T. G. Allen, E. Van Kerschaver, M. I. Saidaminov, D. Baran, Q. Qiao, K. Zhu, S. De Wolf and E. H. Sargent, *Science*, 2020, **367**, 1135.
7 L. Meng, J. You, T.-F. Guo, Y. Yang, *Acc. Chem. Res.*, 2016, **49**, 155.
8 (a) M. Wang, W. Li, H. Wang, K. Yang, X. Hu, K. Sun, S. Lu, Z. Zang, *Adv. Electron. Mater.*, 2020, **6**, 2000604; (b) W. Li, H. Wang, X. Hu, W. Cai, C. Zhang, M. Wang, Z. Zang, Sol. RRL, 2021, 5, 2000573.
9 M. Stolterfoht, C. M. Wolff, J. A. Márquez, S. Zhang, C. J. Hages, D. Rothhardt, S. Albrecht, P. L. Burn, P. Meredith, T. Unold and D. Neher, *Nat. Energy*, 2018, **3**, 847.
10 M. Wang, H. Wang, W. Li, X. Hu, K. Sun, Z. Zang, *J. Mater. Chem. A*, 2019, 7, 26421.
11 A. Magomedov, A. Al-Ashouri, E. Kasparavičius, S. Strazdaite, G. Niaura, M. Jošt, T. Malinauskas, S. Albrecht and V. Getautis, *Adv. Energy Mater*, 2018, **8**, 1801892.
12 C. Wang, J. Hu, C. Li, S. Qiu, X. Liu, L. Zeng, C. Liu, Y. Mai and F. Guo, *Sol. RRL*, 2019, **4**, 1900389.
13 K. Rakstys, M. Stephen, J. Saghaei, H. Jin, M. Gao, G. Zhang, K. Hutchinson, A. Chesman, P. L. Burn, I. Gentle and P. E. Shaw, *ACS Appl. Energy Mater.*, 2020, **3**, 889.
14 D. Vaitukaitytė, A. Al-Ashouri, M. Daškevičienė, E. Kamarauskas, J. Nekrasovas, V. Jankauskas, A. Magomedov, S. Albrecht and V. Getautis, *Sol. RRL*, 2021, **5**, 2000597.
15 S.-i. Kato, H. Noguchi, A. Kobayashi, T. Yoshihara, S. Tobita and Y. Nakamura, *J. Org. Chem.*, 2012, **77**, 9120.
16 B. Wex and B. R. Kaafarani, *J. Mater. Chem. C*, 2017, **5**, 8622.
17 M. Reig, J. Puigdollers and D. Velasco, *J. Mater. Chem. C*, 2015, **3**, 506.
18 J. An, X. Yang, B. Cai, L. Zhang, K. Yang, Z. Yu, X. Wang, A. Hagfeldt and L. Sun, *ACS Appl. Mater. & Interfaces*, 2020, **12**, 46397.
19 S. Zhou, M. Daskeviciene, M. Steponaitis, G. Bubniene, V. Jankauskas, K. Schutt, P. Holzhey, A. R. Marshall, P. Caprioglio, G. Christoforo, J. M. Ball, T. Malinauskas, V. Getautis and H. J. Snaith, *Sol. RRL*, 2022, **6**, 2100984.
20 A. Matoliukstyte, E. Burbulis, J. V. Gražulevičius, V. Gaidelis and V. Jankauskas, Synth. Met., 2008, 158(11), 462.

